Nano Research
2022, 15(6): 5483–5491

ISSN 1998-0124 CN 11-5974/O4
https://doi.org/10.1007/s12274-022-4164-2

Research Article

Multiple detection of 15 triazine herbicides by gold nanoparticle based-paper sensor

Lingling Guo[1,2], Xinxin Xu[1,2], Jing Zhao[3], Shudong Hu[3], Liguang Xu[1,2], Hua Kuang[1,2] (✉), and Chuanlai Xu[1,2] (✉)

[1] *State Key Laboratory of Food Science and Technology, Jiangnan University, Wuxi 214122, China*
[2] *International Joint Research Laboratory for Biointerface and Biodetection, and School of Food Science and Technology, Jiangnan University, Wuxi 214122, China*
[3] *Department of Radiology, Affiliated Hospital, Jiangnan University, Wuxi 214122, China*

Received: 16 November 2021 / **Revised:** 30 December 2021 / **Accepted:** 17 January 2022

ABSTRACT

Triazine herbicides have been widely used in agriculture, but their residues can harm the environment and human health. To help monitor these, we have developed an effective immunochromatographic strip test that can simultaneously detect 15 different triazines in grain samples (including ametryn, cyprazine, atraton, prometon, prometryn, atrazine, propazine, terbuthylazine, simetryn, trietazine, secbumeton, simazine, desmetryn, terbumeton and simetone). Based on our optimization procedure, the visual limit of detection (vLOD) for these triazines was found to be 2–10 ng/mL in assay buffer, and 0.02–0.1 mg/kg in grain samples. Four different grain matrices including corn, brown rice, wheat, and sorghum were studied and the test results showed no significant differences between the 15 triazines analyzed using this method. This test is simple, convenient, rapid, and low-cost, and could be an effective tool for primary screening of triazine residues in grain samples.

KEYWORDS

triazine herbicides, immunochromatographic strip, gold nanoparticles, grain

1 Introduction

Triazine-based herbicides are used world-wide for the control of annual grasses and broadleaf weeds in various crops, and account for an estimated 30% of agricultural herbicides [1]. Triazine herbicides have a common triazine ring (Fig. 1(a)), and depending on the substituent groups of X, they can be generally divided into three categories. The first group includes atrazine, cyprazine, propazine, terbutylazine, trietazine and simazine, whose X is Cl. The second group, in which X is O-CH_3, includes atraton, prometon, secbumeton, terbumeton and simetone. The third group includes ametryn, prometryn, simetryn, and desmetryn, whose X is S-CH_3. They have the characteristics of high mobility, persistence, and low degradation rate in the environment. Their widespread and excessive use have led to serious accumulation in soil and water, and they can be transferred directly or indirectly to human body through food chain. Several reports demonstrated that exposure to triazine herbicides could cause the disorder of reproductive system, nervous system, and immune system of mammals [2–4].Consequently, many countries have set maximum residue limits (MRLs) for agricultural products according to the actual usage. Take atrazine for example, China enforces MRLs of 0.05 mg/kg for sorghum, corn and millet; but in Japan, the MRLs are 0.2 mg/kg in corn and 0.3 mg/kg in wheat. Based on the details mentioned above, it is important to develop effective detection methods to police this.

Instrumental analytical methods, such as gas chromatography-tandem mass spectrometry [5] and high performance liquid chromatography-tandem mass spectrometry (HPLC-MS/MS) [6–8], are the standard methods used for the detection of triazine residues. Although these methods are highly accurate, sensitive and reliable, some disadvantages such as the need for large amounts of organic solvents, complicated sample pre-processing steps, bulky instrumentation, long detection time, high cost and the need for professional operators, make them not suitable for on-site detection.

In contrast, immunoassays such as enzyme-linked immunosorbent assay (ELISA) and immunochromatographic assay (ICA), are time saving, convenient and economic, and they have been widely applied to food quality control [9–15], disease diagnosis [16–25] and environmental pollutant analysis [26–30]. Several immunoassays have also been developed for the determination of triazines (Table 1) [31–37]. These methods are all based on the use of a specific antibody (monoclonal antibody, polyclonal antibody, or antisera) against antigen. Enzymes (goat anti-mouse IgG horseradish peroxidase) or nanoparticles (gold nanoparticles (GNPs), up-conversion materials, or mesoporous core–shell palladium@platinum nanoparticles) have all been used for signal visualization and amplification before detection [38–40]. Due to their advantage as visual detection systems, these methods need no specialist equipment and are of low cost. Furthermore, ICAs are more suitable for rapid detection than other types of immunoassays [41, 42]. However, current ICAs can only detect one type of triazine rather than multiple forms.

In this work, we prepared a GNP based-immunochromatographic strip for the multiple determination of 15 triazine herbicides using a series of optimization steps. Furthermore, its usefulness with different grains (corn, brown rice, wheat, and sorghum) and the effects of different grain matrices were also determined.

Address correspondence to Hua Kuang, kuangh@jiangnan.edu.cn; Chuanlai Xu, xcl@jiangnan.edu.cn

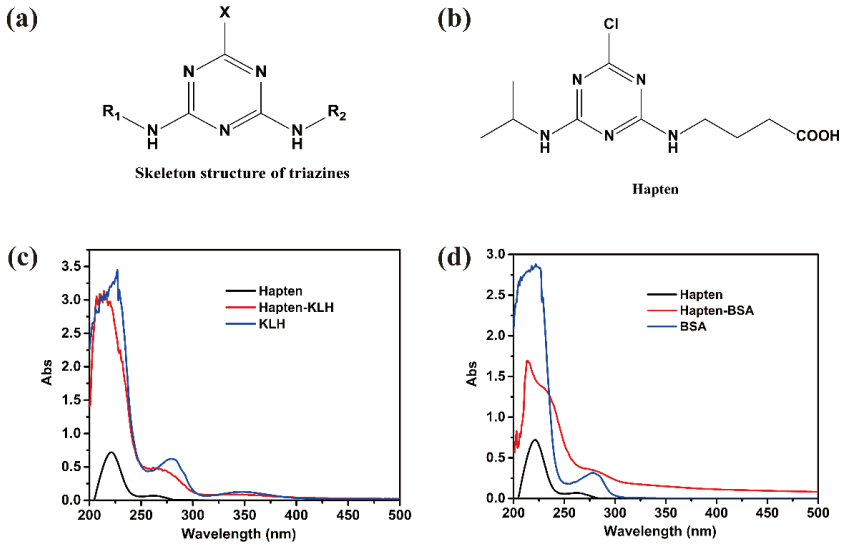

Figure 1 (a) Skeleton structure of triazines; (b) chemical structure of hapten; (c) UV–vis spectra of Hapten, KLH, and Hapten-KLH; (d) UV–vis spectra of Hapten, BSA, and Hapten-BSA.

Table 1 Immunoassays for triazines herbicides detection

Method	Recognition material	Label	Targets	Matrix	Ref.
ELISA	PcAb	HRP	11 triazines	Water	[31]
ELISA	PcAb	HRP	10 triazines	Ginger	[32]
ICA	Antisera	GNPs	Atrazine	Apple and blackcurrant juices	[33]
Fluorescence immunoassay	PcAb	Upconversion nanoparticles	Atrazine	Corn, rice, sugar cane juice and river water	[34]
Electrochemical method	MAb	Pd@Pt nanoparticles	Atrazine and acetochlor	Water	[35]
ICA	MAb	GNPs	Atrazine	Herb	[36]
ICA	MAb	GNPs	Prometryn	Herb	[37]

2 Materials and methods

2.1 Reagents and apparatus

Triazine standards (ametryn, cyprazine, atraton, prometon, prometryn, atrazine, propazine, terbuthylazine, simetryn, trietazine, secbumeton, simazine, desmetryn, terbumeton, simetone, cyanazine, dipropetryn and metribuzin) were purchased from TanMo Quality Testing Technology Co., Ltd (Beijing, China). Goat anti-mouse IgG antibody, keyhole limpet hemocyanin (KLH), bovine serum albumin (BSA) and chloroauric acid ($HClO_4$) were obtained from Sigma-Aldrich (St. Louis, MO, USA). 4-((4-chloro-6-(isopropylamino)-1,3,5-triazin-2-yl)amino)butanoic acid was prepared by Sandia Pharmaceutical Technology (Shanghai) Co., LTD.

Nitrocellulose (NC) membrane was purchased from Sartorius Stedim Biotech GmbH (Gőttingen, Germany). Sample pad, absorption pad, glass fiber anline-height-add:-0.5ptd polyvinychloride (PVC) backing plates were purchased from JieYi Biotechnology Co., Ltd. (Shanghai, China) and the *XYZ* dispensing platform and guillotine cutting module for immunochromatographic strip preparation were from Shanghai Kinbio Tech Co., Ltd.

2.2 Antigen and monoclonal antibody preparation

According to a previous report [31], 4-((4-chloro-6-(isopropylamino)-1,3,5-triazin-2-yl)amino)butanoic acid were used as hapten (Fig. 1(b)). Immunogen (Hapten-KLH) and coating antigen (Hapten-BSA) were prepared by the active ester method [43]. Through immunization, cell fusion, and ascites purification, anti-triazine monoclonal antibody (mAb) was obtained.

2.3 Preparation and characterization of GNPs

GNPs were prepared according to our previous study [43, 44]. Briefly, 12.5 mL, 10 mmol/L $HClO_4$ solution was added to 487.5 mL ultrapure water. After boiling and constant stirring for 15 min, 1 mL of sodium citrate tribasic dihydrate (10%, w/v) was added quickly. Then the solution was boiled until it turned to a red-wine color (approximately 30 min) and allowed to cool to room temperature and kept at 4 °C for further use. The prepared GNP solution was characterized using an ultraviolet–visible (UV–vis) spectrophotometer and transmission electron microscope (TEM).

2.4 Synthesis of the GNP-mAb conjugate

The GNP-labelled mAb was prepared as follows [45–47]. First, K_2CO_3 (0.2 mol/L) was used to adjust the pH of the GNP solution (10 mL) to 8.2. Then, the anti-triazine mAb diluted with 0.2 mol/L borate saline buffer (BSB) was added at room temperature. After 1 h at room temperature, 0.5 mL of BSA solution (10%, w/v) was added to the solution to block any unbound site. 2 h later, the solution was centrifuged at 4 °C, 8,000 g for 55 min to remove unconjugated mAb. The supernatant was then removed and the pellet was resuspended in 10 mL of resuspension solution. This was added into a microwell plate (50 μL/well). The solution was finally lyophilized using a vacuum freeze-dryer, and stored in a drying cabinet until use.

2.5 Construction of the ICA strips

This ICA strip was composed of a sample pad, an absorbent pad, and a NC membrane with a PVC backing plate, and was assembled in layers (Fig. 2). The NC membrane was placed on the

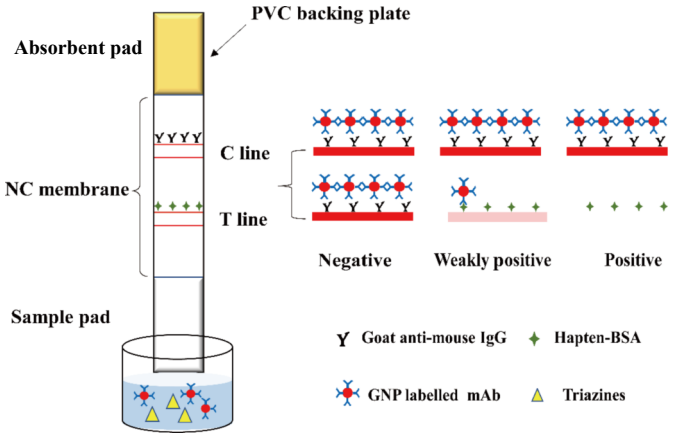

Figure 2 Schematic diagram and test principle of ICA.

center of the PVC backing plate and then the sample pad and absorbent pad were stuck to either end and overlapped with the NC membrane by 2 mm. Then Hapten-BSA and goat anti-mouse IgG antibody were sprayed onto the NC membrane forming the test T and control C lines. After drying for 2 h at 37 °C, it was cut into strips of 2.95 mm in width and then stored in a drying cabinet at room temperature until use.

2.6 Analysis of grain samples by ICA

2.6.1 ICA procedure

For the ICA test, 200 μL of standard or sample solution was added into a microwell plate containing freeze-dried GNP-labelled mAb. 2 min later, the ICA strip was placed into the well. Due to capillarity action, the solution flowed from the sample pad to the absorbent pad, and after 4 min, the strip was removed and the color of the T line was observed.

2.6.2 Sample pretreatment

1 g of crushed grain sample was extracted with 4 mL of extraction solution with vibration for 3 min. After centrifugation at 3,000 g for 3 min, the supernatant was removed and diluted using a sample diluent for ICA analysis.

2.6.3 Matrix effects

Different triazines-negative grain samples (purchased from a local supermarket: corn, wheat, brown rice, and sorghum) were confirmed by UPLC-MS/MS. Details of the UPLC-MS/MS method are given in the Electronic Supplementary Material (ESM), including liquid chromatography (LC) and mass spectrometry (MS) conditions (Table S1) and MS/MS parameters (Table S2 in the ESM). Triazine standard solutions at different concentrations (0, 0.02, 0.1, 0.5, and 2.5 mg/kg) were spiked into the negative grain samples for ICA analysis after the pretreatment described above.

3 Results and discussion

3.1 Characterization of antigen and mAb

Hapten-KLH and Hapten-BSA were conjugated successfully and characterized by ultraviolet (UV) spectrum (Figs. 1(c) and 1(d)), which had both the characteristic UV absorption peaks of Hapten and carrier protein (KLH or BSA).

The half-maximal inhibition concentration values (IC_{50}) of 15 triazines were tested by ELISA [31]. As shown in Table 2, this prepared mAb can recognize 15 triazines. The mainly reason is that the hapten retained the common structure in maximum, and meanwhile the space arm (-NH-CH_2-CH_2-CH_2-CO-) is good for the exposure of the common structure to produce group-selective monoclonal antibody.

3.2 Characterization of GNPs

Due to their high specific surface area, chemical inertness and biocompatibility, GNPs are one of the most attractive materials for use as a label for detecting analytes with an ICA, and can provide a visual signal on the T line when binding between antibody and antigen occurs.

Herein, we have adopted the classical citrate reduction method for the synthesis of GNPs [48], and citrate ions not only act as a reducing agent for the GNP formation, but also play a role in preventing the GNPs from aggregating [49]. With this method, the amount of citrate is related to the GNP size and GNPs of 10–40 nm in diameter are reported to be optimal for ICA analysis, as smaller particles have unacceptable color development and larger particles are unstable for long-term storage [50]. Based on our previous research [51], GNPs with a diameter of 15 nm were found to be stable and the wine color produced was suitable for ICA analysis. As shown in Fig. 3(a) under the TEM, our GNPs appeared uniform and well dispersed and the UV–vis spectrophotometer in Fig. S1 in the ESM showed a strong absorption peak at 520 nm, which is also consistent with previous reports.

3.3 GNP labeled mAb

The preparation of GNP labeled mAb mainly utilizes electrostatic adsorption between the negatively charged surface of the GNPs and the positively charged groups on the mAb. This bioconjugation is highly susceptible to pH when the pH of the system is greater than or equal to the isoelectric point of mAb (pH 8.0), and the GNP labeled mAb has good stability. Thus, the amount of K_2CO_3 used for the adjustment of pH needs be optimized.

According to a previous report [52], the optimum amount of K_2CO_3 used for the labelling process is also defined as the minimum amount preventing GNP accumulation under the addition of 10% NaCl (w/w). As can be seen from Fig. S2 in the ESM, when the K_2CO_3 content in GNP solution was lower than 5 μL/mL, the particles began to clump, and the color of the solution turned very dark. When the K_2CO_3 content was greater than or equaled 5 μL/mL, the particles were well dispersed. Furthermore, excess K_2CO_3 may also influence the conjugation of mAb and GNPs, which is illustrated in Fig. 3(b). We can see that the color of the T line was darker when K_2CO_3 content was 5 μL/mL.

The amount of mAb used was also optimized and herein an increase in mAb concentration also gave a darker T line, and when the mAb content in GNP solution was 10 μg/mL the T line

Table 2 Structures and vLODs of 15 triazine herbicides tested by ICA strip

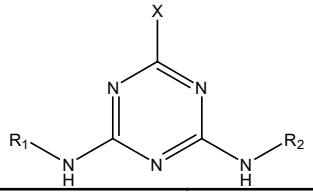

Number	Chemical	X	R_1	R_2	IC_{50} (ng/mL)	vLOD (mg/kg) in grain	vLOD (ng/mL) in buffer
1	Ametryn	S-CH_3	$CH(CH_3)_2$	CH_2CH_3	1.90	0.1	10
2	Cyprazine	Cl	$CH(CH_3)_2$		0.36	0.02	2
3	Atraton	O- CH_3	$CH(CH_3)_2$	CH_2CH_3	0.60	0.02	2
4	Prometon	O- CH_3	$CH(CH_3)_2$	$CH(CH_3)_2$	0.35	0.02	2
5	Prometryn	S-CH_3	$CH(CH_3)_2$	$CH(CH_3)_2$	2.10	0.1	10
6	Atrazine	Cl	$CH(CH_3)_2$	CH_2CH_3	0.48	0.02	2
7	Propazine	Cl	$CH(CH_3)_2$	$CH(CH_3)_2$	0.60	0.02	2
8	Terbutylazine	Cl	CH_2CH_3	$C(CH_3)_3$	0.52	0.02	2
9	Simetryn	S-CH_3	CH_2CH_3	CH_2CH_3	1.90	0.1	10
10	Trietazine	Cl	$(CH_2CH_3)_2$	CH_2CH_3	2.70	0.1	10
11	Secbumeton	O- CH_3	CH_2CH_3	$CH_3CH(CH_2CH_3)$	3.00	0.1	10
12	Simazine	Cl	CH_2CH_3	CH_2CH_3	0.44	0.1	2
13	Desmetryn	S-CH_3	CH_3	$CH(CH_3)_2$	0.60	0.1	2
14	Terbumeton	O- CH_3	CH_2CH_3	$C(CH_3)_3$	0.50	0.1	2
15	Simetone	O- CH_3	CH_2CH_3	CH_2CH_3	1.82	0.1	10

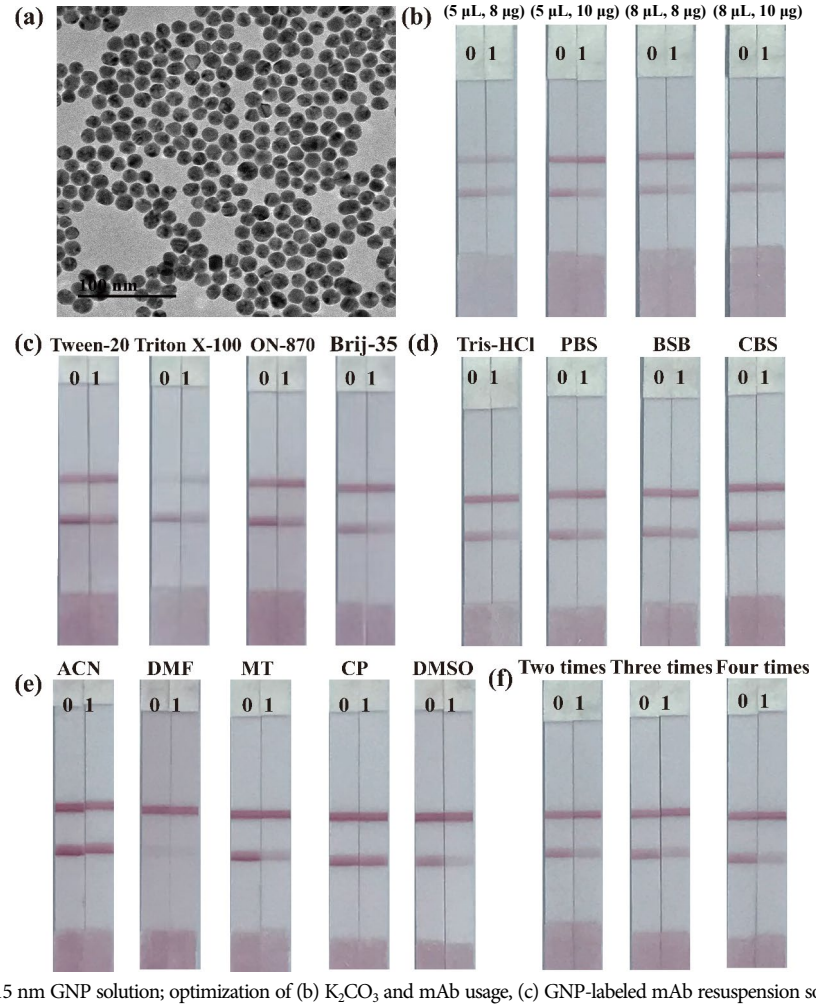

Figure 3 (a) TEM images of 15 nm GNP solution; optimization of (b) K_2CO_3 and mAb usage, (c) GNP-labeled mAb resuspension solution, (d) ICA assay buffer, (e) organic solvents for sample extraction, and (f) sample dilution ratio for ICA analysis. In (b)–(d), 0 = blank and 1 = 20 ng/mL of ametryn standard solution; in (e) and (f), 0 = blank and 1 = 0.1 mg/kg of ametryn in corn.

color became maximally dark. The inhibition when ametryn (20 ng/mL) was added was also distinct. Besides, the gray values (T line and C line) obtained by processing strip images using Photoshop software could further confirm the result. The gray value was not very different, but the inhibition ratio was better under the condition of 5 μL of K_2CO_3 and 10 μg of mAb (Table S3 in the ESM).

Thus, 5 μL/mL K_2CO_3 and 10 μg/mL mAb were chosen for the labeling of the mAb with the GNPs.

3.4 ICA development

3.4.1 ICA principle

The principle of the ICA is based on the competition between the fixed antigen on the T line and the free analytes in the sample solution for binding to the GNP labeled mAb, as shown in Fig. 2. For weakly positive or positive samples, the analyte in the sample solution firstly conjugates with the GNP labeled mAb during incubation. Due to its capillary effect, the sample solution flows from the sample pad to absorption pad and when it reaches the T line, the unconjugated or non-additional GNP labeled mAb can conjugate with the Hapten-BSA on the T line, making the color of the T line light or even disappear. The C line should always be red because of the binding between the goat anti-mouse IgG and the GNP labelled mAb. For negative samples, no analyte in sample solution conjugates with the GNP labelled mAb, so the T line color is the same as or darker than that of the C line.

3.4.2 Optimization of the ICA

The resuspension solution for the GNP labelled mAb and assay buffer was optimized for ICA analysis. Surfactants play an important role in ICA analysis, and can improve their performance by facilitating sample flow along the strip and increasing the analyte solubility. In this study, the GNP labeled mAb was resuspended in suspension buffer (0.01 M phosphate buffer saline (PBS) solution containing 5% trehalose, 0.2% BSA and 0.04% sodium azide), which was mixed with four different surfactants: 5% Tween-20, 5% Triton X-100, 5% ON-870 and 5% Brij-35. Based on the color intensity at 0 and 20 ng/mL for ametryn in 0.01 M, pH 7.4 PBS, the most stable deep red was obtained using Brij-35 (Fig. 3(c) and Table S3 in the ESM).

Assay buffers at different pH and ionic strengths can also influence the binding of the antibody and antigen, and further affect the sensitivity of the ICA. Thus, four kinds of assay buffer, including tris(hydroxymethyl)aminomethane hydrochloride solution (Tris-HCl, pH 6.0), PBS (pH 7.4), BSB (pH 8.2) and carbonate buffer solution (CBS, pH 9.6), with the same concentration (0.01 M) and Brij-35 content (3%, w/w), were optimized. The darkest red color on the T line was produced using CBS, but the inhibition with the addition of ametryn (20 ng/mL) was less obvious than that seen with PBS (Fig. 3(d) and Table S3 in the ESM). While the color intensities in Tris-HCl and BSB were slightly lower than that for PBS. Therefore, PBS (0.01 M, pH 7.4) was chosen as the assay buffer for triazine analysis.

Based on the optimization of 15 types of triazines, including ametryn, cyprazine, atraton, prometon, prometryn, atrazine, propazine, terbuthylazine, simetryn, trietazine, secbumeton, simazine, desmetryn, terbumeton and simetone, we used ICA for their determination. The standard concentrations of each triazine used were 0, 2, 10, 50 and 250 ng/mL and from the original strip images (Fig. 4), we can determine the visual limit of detection (vLOD) for each triazine, which is defined as the concentration, at which the T line color is obviously less than that of the blank solution. The vLOD values in buffer for cyprazine, atraton, prometon, atrazine, propazine, terbuthylazine, simazine,

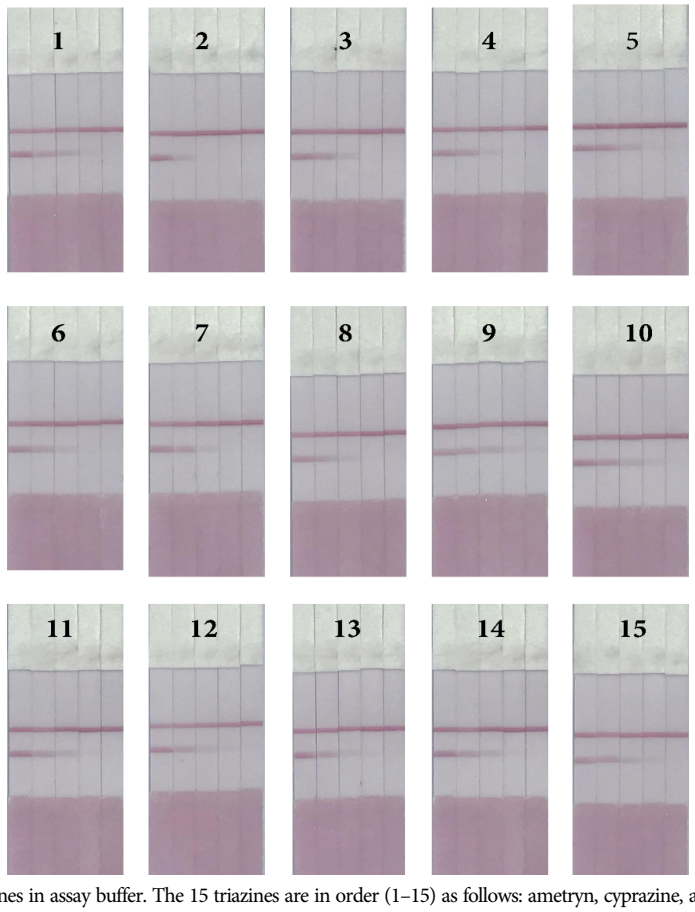

Figure 4 The strip images of 15 triazines in assay buffer. The 15 triazines are in order (1–15) as follows: ametryn, cyprazine, atraton, prometon, prometryn, atrazine, propazine, terbuthylazine, simetryn, trietazine, secbumeton, simazine, desmetryn, terbumeton and simetone. The standard concentrations of each triazine are 0, 2, 10, 50 and 250 ng/mL from left to right.

desmetryn, and terbumeton were all 2 ng/mL, and the other triazines including ametryn, prometryn, simetryn, trietazine, secbumeton, and simetone were all 10 ng/mL (Table 2). Furthermore, three other triazines (cyanazine, dipropetryn and metribuzin) were also tested, which showed no obvious color change at a concentration of 5,000 ng/mL (Fig. S3 in the ESM), suggesting that the strips could not be used to detect cyanazine, dipropetryn and metribuzin.

3.5 Analysis of spiked grain samples by ICA

3.5.1 *Sample extraction solution*

Different organic solvents can influence not only the extraction efficiency but also the binding of antigen to antibody. Five organic solvents, including acetonitrile (ACN), dimethyl formamide (DMF), methanol (MT), acetone (CP) and dimethylsulfoxide (DMSO), were optimized, as shown in Fig. 3(e); the order of the color intensity in the blank sample was shown to be DMF < DMSO < CP < MT < ACN and the order of inhibition for the spiked sample (0.1 mg/kg ametryn) was MT > DMSO > CP > ACN. However, the inhibition when using DMF as the extraction solvent was not clear because it was invisible to the naked eye. Because of these tests, MT with the highest color intensity and inhibition was chosen as the solution to be used for the grain extraction when using the ICA.

3.5.2 *Sample dilution multiple*

An appropriate sample dilution can reduce the interference between MT and the grain matrix in the ICA. The color strips with blank and spiked samples (0.1 mg/kg of ametryn in corn extracting solution) had almost identical color intensities when diluted two, three, and four times, respectively (Fig. 3(f)). This result suggested that our developed ICA based on a triazines–mAb had the characteristics of grain matrix resistance. And high dilution ratio signified low sensitivity. Thus, grains samples were diluted two times for triazine residue detection.

3.5.3 *Matrix effects*

Four grain samples, including corn, wheat, brown rice, and sorghum, purchased from thr local supermarket were triazines-negative, which can be seen from the chromatograms of the quantitative ions for the 15 triazines from 1 ng/mL standard solution and four grain samples (Fig. 5).

Matrix effects were evaluated based on the vLOD values of the four types of grains spiked with the 15 different triazines after a pretreatment and analysis as described above. From the original strip images for the spiked corn samples (Fig. 6), the vLOD values for cyprazine, atraton, prometon, atrazine, propazine, and terbuthylazine, were all 0.02 mg/kg, and the other triazines including ametryn, prometryn, simetryn, trietazine, secbumeton,

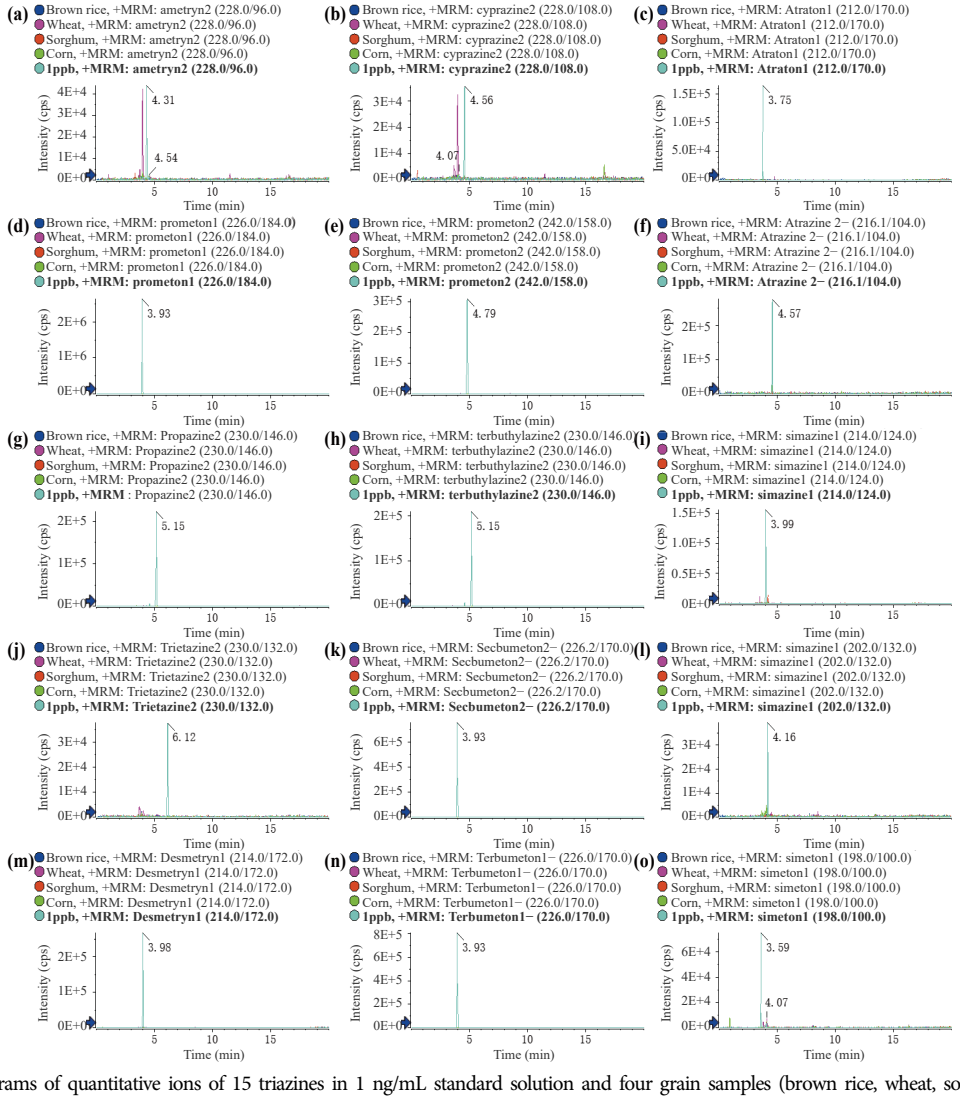

Figure 5 Chromatograms of quantitative ions of 15 triazines in 1 ng/mL standard solution and four grain samples (brown rice, wheat, sorghum and corn): (a) ametryn, (b) cyprazine, (c) atraton, (d) prometon, (e) prometryn, (f) atrazine, (g) propazine, (h) terbuthylazine, (i) simetryn, (j) trietazine, (k) secbumeton, (l) simazine, (m) desmetryn, (n) terbumeton and (o) simetone.

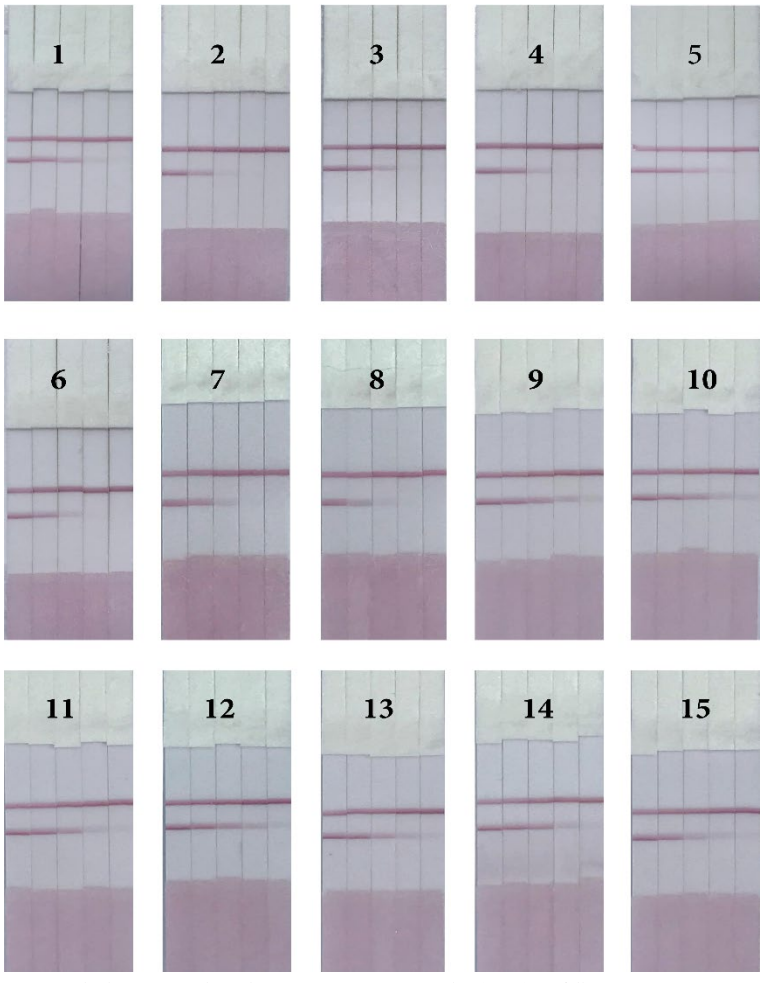

Figure 6 Strip images of 15 triazines in spiked corn samples. The 15 triazines are in order (1–15) as follows: ametryn, cyprazine, atraton, prometon, prometryn, atrazine, propazine, terbuthylazine, simetryn, trietazine, secbumeton, simazine, desmetryn, terbumeton and simetone. The spiked concentrations of each triazine are 0, 0.02, 0.1, 0.5 and 2.5 mg/kg from left to right.

simazine, desmetryn, terbumeton and simetone, were all 0.1 mg/kg. Moreover, when comparing the strip results (Figs. S4–S6 in the ESM), we found that each triazine had the same vLOD values in corn maize, brown rice, wheat and sorghum, indicating that the result with the developed ICA strips is not affected by grain matrices. Thus, our assembled ICA strips can be used for the detection of 15 triazines simultaneously from grain samples, and the test results are consistent between different grain types. The vLOD values for the 15 triazines in grain are listed in Table 2. Except for prometryn with an MRL of 0.02 mg/kg in corn and simetryn with an MRL of 0.05 mg/kg in brown rice, all the other triazine vLOD values satisfy Chinese MRL requirements. Compared with single-residue ICA previously reported, this developed multi-residue ICA cannot quantitate triazines, but it has advantages of high detection efficiency, low cost and short detection time. Furthermore, the whole testing process including pretreatment was no more than 15 min. Conclusively, this technique represents a simple-to-operate and lower-cost assay and is suitable for the fast screening of triazine residues in various grain samples.

4 Conclusion

Herein, we have successfully prepared rapid detection strips and developed an ICA for the rapid and simultaneous detection of 15 different triazines in grain samples, and our results showed no significant differences between different grain matrices. Moreover, the whole operation is convenient and simple, and can be completed within 15 min. Thus, the developed ICA can provide a rapid, low-cost, and efficient tool for the on-site determination of triazine herbicides in grain samples.

Acknowledgements

This work was financially supported by the National Key R&D Program (No. 2019YFC1604703) and the Natural Science Foundation of Jiangsu Province (Nos. BK20200598, CMB21S1614, and CSE11N1310).

Electronic Supplementary Material: Supplementary material (UV–vis spectra of 15 nm-GNP; K_2CO_3 usage; cross reactivity; strip images for spiked rice, wheat and sorghum samples, UPLC-MS/MS parameters; gray values for strip optimization) is available in the online version of this article at https://doi.org/10.1007/s12274-022-4164-2.

References

[1] Fingler, S.; Mendaš, G.; Dvoršćak, M.; Stipičević, S.; Vasilić, Ž.; Drevenkar, V. Herbicide micropollutants in surface, ground and drinking waters within and near the area of Zagreb, Croatia. *Environ. Sci. Pollut. Res.* **2017**, *24*, 11017–11030.

[2] Parker, E. T.; Owen, M. D. K.; Bernards, M. L.; Curran, W. S.; Steckel, L. E.; Mueller, T. C. A comparison of symmetrical and asymmetrical triazine herbicides for enhanced degradation in three midwestern soils. *Weed Sci.* **2018**, *66*, 673–679.

[3] Saka, M.; Tada, N.; Kamata, Y. Chronic toxicity of 1, 3, 5-triazine herbicides in the postembryonic development of the western clawed

frog *Silurana tropicalis*. *Ecotoxicol. Environ. Saf.* **2018**, *147*, 373–381.
[4] Rimayi, C.; Odusanya, D.; Weiss, J. M.; de Boer, J.; Chimuka, L. Seasonal variation of chloro-s-triazines in the Hartbeespoort Dam catchment, South Africa. *Sci. Total Environ.* **2018**, *613−614*, 472–482.
[5] Brandhonneur, N.; De Sousa Mendes, M.; Lepvrier, E.; Esseiva, E. F.; Chevanne, F.; Le Corre, P. A micro-QuEChERS method coupled to GC-MS for the quantification of pesticides in specific maternal and fetal tissues. *J. Pharm. Biomed. Anal.* **2015**, *104*, 90–96.
[6] Masís-Mora, M.; Beita-Sandí, W.; Rodríguez-Yáñez, J.; Rodríguez-Rodríguez, C. E. Validation of a methodology by LC-MS/MS for the determination of triazine, triazole and organophosphate pesticide residues in biopurification systems. *J. Chromatogr. B* **2020**, *1156*, 122296.
[7] De O. Silva, R.; De Menezes, M. G. G.; De Castro, R. C.; De A. Nobre, C.; Milhome, M. A. L.; Do Nascimento, R. F. Efficiency of ESI and APCI ionization sources in LC-MS/MS systems for analysis of 22 pesticide residues in food matrix. *Food Chem.* **2019**, *297*, 124934.
[8] Wang, S. S.; She, Y. X.; Hong, S. H.; Du, X. W.; Yan, M. M.; Wang, Y. L.; Qi, Y.; Wang, M.; Jiang, W. Y.; Wang, J. Dual-template imprinted polymers for class-selective solid-phase extraction of seventeen triazine herbicides and metabolites in agro-products. *J. Hazard. Mater.* **2019**, *367*, 686–693.
[9] Xiao, X. Y.; Hu, S.; Lai, X. C.; Peng, J.; Lai, W. H. Developmental trend of immunoassays for monitoring hazards in food samples: A review. *Trends Food Sci. Technol.* **2021**, *111*, 68–88.
[10] Poungmalai, P.; Buakeaw, A.; Puthong, S.; Khongchareonporn, N. A specific monoclonal antibody for chlortetracycline detection in milk and honey samples based on ELISA. *Food Agric. Immunol.* **2021**, *32*, 163–173.
[11] Lei, X. L.; Xu, X. X.; Liu, L. Q.; Kuang, H.; Xu, L. G.; Hao, C. L. Immunochromatographic test strip for the rapid detection of tricaine in fish samples. *Food Agric. Immunol.* **2020**, *31*, 687–699.
[12] Li, Y.; Wang, Z. X.; Sun, L.; Liu, L. Q.; Xu, C. L.; Kuang, H. Nanoparticle-based sensors for food contaminants. *TrAC Trends Anal. Chem.* **2019**, *113*, 74–83.
[13] Li, Y.; Liu, L. Q.; Xu, C. L.; Kuang, H.; Sun, L. Integration of antibody-antigen and receptor-ligand reactions to establish a gold strip biosensor for detection of 33 β-lactam antibiotics. *Sci. China Mater.* **2021**, *64*, 2056–2066.
[14] Wang, W. B.; Liu, L. Q.; Song, S. S.; Xu, L. G.; Kuang, H.; Zhu, J. P.; Xu, C. L. Gold nanoparticle-based strip sensor for multiple detection of twelve *Salmonella* strains with a genus-specific lipopolysaccharide antibody. *Sci. China Mater.* **2016**, *59*, 665–674.
[15] Zeng, L.; Xu, X. X.; Song, S. S.; Xu, L. G.; Liu, L. Q.; Xiao, J.; Xu, C. L.; Kuang, H. Synthesis of haptens and gold-based immunochromatographic paper sensor for vitamin B_6 in energy drinks and dietary supplements. *Nano Res.* , in press, DOI: 10.1007/s12274-021-3734-z.
[16] Zeng, L.; Li, Y.; Liu, J.; Guo, L. L.; Wang, Z. X.; Xu, X. X.; Song, S. S.; Hao, C. L.; Liu, L. Q.; Xin, M. G. et al. Rapid, ultrasensitive and highly specific biosensor for the diagnosis of SARS-CoV-2 in clinical blood samples. *Mater. Chem. Front.* **2020**, *4*, 2000–2005.
[17] Yee, E. H.; Lathwal, S.; Shah, P. P.; Sikes, H. D. Detection of biomarkers of periodontal disease in human saliva using stabilized, vertical flow immunoassays. *ACS Sens.* **2017**, *2*, 1589–1593.
[18] Khlebtsov, B. N.; Bratashov, D. N.; Byzova, N. A.; Dzantiev, B. B.; Khlebtsov, N. G. SERS-based lateral flow immunoassay of troponin I by using gap-enhanced Raman tags. *Nano Res.* **2019**, *12*, 413–420.
[19] Pham, X. H.; Hahm, E.; Kim, T. H.; Kim, H. M.; Lee, S. H.; Lee, S. C.; Kang, H.; Lee, H. Y.; Jeong, D. H.; Choi, H. S. et al. Enzyme-amplified SERS immunoassay with Ag-Au bimetallic SERS hot spots. *Nano Res.* **2020**, *13*, 3338–3346.
[20] Yang, J. X.; Wang, C. H.; Shi, S.; Dong, C. Y. Nanotechnologies for enhancing cancer immunotherapy. *Nano Res.* **2020**, *13*, 2595–2616.
[21] Kim, E.; Lim, E. K.; Park, G.; Park, C.; Lim, J. W.; Lee, H.; Na, W.; Yeom, M.; Kim, J.; Song, D. et al. Advanced nanomaterials for preparedness against (Re-)emerging viral diseases. *Adv. Mater.* **2021**, *33*, 2005927.
[22] Zhang, Z. W.; Ma, P.; Ahmed, R.; Wang, J.; Akin, D.; Soto, F.; Liu, B. F.; Li, P. W.; Demirci, U. Advanced point-of-care testing technologies for human acute respiratory virus detection. *Adv. Mater.* **2021**, *34*, 2103646.
[23] Li, S.; Guo, X.; Gao, R.; Sun, M. Z.; Xu, L. G.; Xu, C. L.; Kuang, H. Recent progress on biomaterials fighting against viruses. *Adv. Mater.* **2021**, *33*, 2005424.
[24] Yang, M. Z.; Zhang, W.; Yang, J. C.; Hu, B. F.; Cao, F. J.; Zheng, W. S.; Chen, Y. P.; Jiang, X. Y. Skiving stacked sheets of paper into test paper for rapid and multiplexed assay. *Sci. Adv.* **2017**, *3*, eaao4862.
[25] Ates, H. C.; Brunauer, A.; von Stetten, F.; Urban, G. A.; Güder, F.; Merkoçi, A.; Früh, S. M.; Dincer, C. Integrated devices for non-invasive diagnostics. *Adv. Funct. Mater.* **2021**, *31*, 2010388.
[26] Li, C. W.; Wei, Y. L.; Zhang, S. T.; Tan, W. L. Advanced methods to analyze steroid estrogens in environmental samples. *Environ. Chem. Lett.* **2020**, *18*, 543–559.
[27] Yu, X. T.; Zhang, X.; Xu, J. J.; Guo, P. Y.; Li, X. M.; Wang, H.; Xu, Z. L.; Lei, H. T.; Shen, X. Generation of recombinant antibodies by mammalian expression system for detecting S-metolachlor in environmental waters. *J. Hazard. Mater.* **2021**, *418*, 126305.
[28] Ling, S. M.; Zhao, Q.; Iqbal, M. N.; Dong, M. K.; Li, X. L.; Lin, M.; Wang, R. Z.; Lei, F. Y.; He, C. Z.; Wang, S. H. Development of immunoassay methods based on monoclonal antibody and its application in the determination of cadmium ion. *J. Hazard. Mater.* **2021**, *411*, 124992.
[29] Duan, J. L.; Zhan, J. H. Recent developments on nanomaterials-based optical sensors for Hg^{2+} detection. *Sci. China Mater.* **2015**, *58*, 223–240.
[30] Huang, P.; Tu, D. T.; Zheng, W.; Zhou, S. Y.; Chen, Z.; Chen, X. Y. Inorganic lanthanide nanoprobes for background-free luminescent bioassays. *Sci. China Mater.* **2015**, *58*, 156–177.
[31] Yuan, M.; Na, Y.; Li, L. L.; Liu, B.; Sheng, W.; Lu, X. N.; Kennedy, I.; Crossan, A.; Wang, S. Computer-aided molecular modeling study on antibody recognition of small molecules: An immunoassay for triazine herbicides. *J. Agric. Food. Chem.* **2012**, *60*, 10486–10493.
[32] Liu, C. M.; Dou, X. W.; Zhang, L.; Kong, W. J.; Wu, L.; Duan, Y. P.; Yang, M. H. Development of a broad-specificity antibody-based immunoassay for triazines in ginger and the quantitative structure–activity relationship study of cross-reactive molecules by molecular modeling. *Anal. Chim. Acta* **2018**, *1012*, 90–99.
[33] Byzova, N. A.; Urusov, A. E.; Zherdev, A. V.; Dzantiev, B. B. Multiplex highly sensitive immunochromatographic assay based on the use of nonprocessed antisera. *Anal. Bioanal. Chem.* **2018**, *410*, 1903–1910.
[34] Sheng, W.; Shi, Y. J.; Ma, J.; Wang, L. L.; Zhang, B.; Chang, Q.; Duan, W. X.; Wang, S. Highly sensitive atrazine fluorescence immunoassay by using magnetic separation and upconversion nanoparticles as labels. *Microchim. Acta* **2019**, *186*, 564.
[35] Ruan, X. F.; Wang, Y. J.; Kwon, E. Y.; Wang, L. M.; Cheng, N.; Niu, X. H.; Ding, S. C.; Van Wie, B. J.; Lin, Y. H.; Du, D. Nanomaterial-enhanced 3D-printed sensor platform for simultaneous detection of atrazine and acetochlor. *Biosens. Bioelectron.* **2021**, *184*, 113238.
[36] Wang, Y. D.; Qin, J. A.; Wu, L.; Wang, B. M.; Eremin, S.; Yang, S. H.; Yang, M. H. Enzyme-linked immunosorbent assay and immunochromatographic strip for rapid detection of atrazine in three medicinal herbal roots. *World J. Tradit. Chin. Med.* **2021**, *7*, 97–103.
[37] Liu, C. M.; Wang, Y. D.; Zhang, L.; Qin, J. A.; Dou, X. W.; Fu, Y. W.; Li, Q.; Zhao, X.; Yang, M. H. An integrated strategy for rapid on-site screening and determination of prometryn residues in herbs. *Anal. Bioanal. Chem.* **2020**, *412*, 621–633.
[38] Usha, S. P.; Manoharan, H.; Deshmukh, R.; Álvarez-Diduk, R.; Calucho, E.; Sai, V. V. R.; Merkoçi, A. Attomolar analyte sensing techniques (AttoSens): A review on a decade of progress on chemical and biosensing nanoplatforms. *Chem. Soc. Rev.* **2021**, *50*, 13012–13089.

[39] Liu, X. L.; Pan, Y. C.; Yang, J. J.; Gao, Y. F.; Huang, T.; Luan, X. W.; Wang, Y. Z.; Song, Y. J. Gold nanoparticles doped metal-organic frameworks as near-infrared light-enhanced cascade nanozyme against hypoxic tumors. *Nano Res.* **2020**, *13*, 653–660.
[40] Bumbudsanpharoke, N.; Ko, S. Nanomaterial-based optical indicators: Promise, opportunities, and challenges in the development of colorimetric systems for intelligent packaging. *Nano Res.* **2019**, *12*, 489–500.
[41] Liu, X. Y.; Wu, W. J.; Cui, D. X.; Chen, X. Y.; Li, W. W. Functional micro-/nanomaterials for multiplexed biodetection. *Adv. Mater.* **2021**, *33*, 2004734.
[42] Tu, J. B.; Torrente-Rodríguez, R. M.; Wang, M. Q.; Gao, W. The era of digital health: A review of portable and wearable affinity biosensors. *Adv. Funct. Mater.* **2020**, *30*, 1906713.
[43] Peng, J.; Liu, L. Q.; Xu, L. G.; Song, S. S.; Kuang, H.; Cui, G.; Xu, C. L. Gold nanoparticle-based paper sensor for ultrasensitive and multiple detection of 32 (fluoro)quinolones by one monoclonal antibody. *Nano Res.* **2017**, *10*, 108–120.
[44] Guo, L. L.; Wu, X. L.; Liu, L. Q.; Kuang, H.; Xu, C. L. Gold nanoparticle‐based paper sensor for simultaneous detection of 11 benzimidazoles by one monoclonal antibody. *Small* **2018**, *14*, 1701782.
[45] Suryoprabowo, S.; Liu, L. Q.; Kuang, H.; Cui, G.; Xu, C. L. Gold immunochromatographic assay for simultaneous detection of sibutramine and sildenafil in slimming tea and coffee. *Sci. China Mater.* **2020**, *63*, 654–659.
[46] Wang, Z. X.; Guo, L. L.; Liu, L. Q.; Kuang, H.; Xu, C. L. Colloidal gold-based immunochromatographic strip assay for the rapid detection of three natural estrogens in milk. *Food Chem.* **2018**, *259*, 122–129.
[47] Chen, Y. N.; Liu, L. Q.; Xu, L. G.; Song, S. S.; Kuang, H.; Cui, G.; Xu, C. L. Gold immunochromatographic sensor for the rapid detection of twenty-six sulfonamides in foods. *Nano Res.* **2017**, *10*, 2833–2844.
[48] Kimling, J.; Maier, M.; Okenve, B.; Kotaidis, V.; Ballot, H.; Plech, A. Turkevich method for gold nanoparticle synthesis revisited. *J. Phys. Chem. B* **2006**, *110*, 15700–15707.
[49] Omidfar, K.; Khorsand, F.; Azizi, M. D. New analytical applications of gold nanoparticles as label in antibody based sensors. *Biosens. Bioelectron.* **2013**, *43*, 336–347.
[50] Khlebtsov, B. N.; Tumskiy, R. S.; Burov, A. M.; Pylaev, T. E.; Khlebtsov, N. G. Quantifying the numbers of gold nanoparticles in the test zone of lateral flow immunoassay strips. *ACS Appl. Nano Mater.* **2019**, *2*, 5020–5028.
[51] Song, S. S.; Suryoprabowo, S.; Liu, L. Q.; Zheng, Q. K.; Wu, X. L.; Kuang, H. Development of an immunochromatographic strip test for rapid detection of sodium nifurstyrenate in fish. *Food Agric. Immunol.* **2019**, *30*, 236–247.
[52] Ma, L.; Wang, S. J.; Xu, D. P.; Xie, M. M.; Ding, C. C.; Tian, Y. C.; Qiu, J. X.; Wang, X.; Dong, Q. L.; Liu, Q. Comparison between gold nanoparticles and FITC as the labelling in lateral flow immunoassays for rapid detection of *Ralstonia solanacearum*. *Food Agric. Immunol.* **2018**, *29*, 1074–1085.